

Technical report 15-029

# **A new emission model including on-ramps for two-class freeway traffic control\***

C. Pasquale, S. Liu, S. Siri, S. Sacone, and B. De Schutter

*If you want to cite this report, please use the following reference instead:*

C. Pasquale, S. Liu, S. Siri, S. Sacone, and B. De Schutter, “A new emission model including on-ramps for two-class freeway traffic control,” *Proceedings of the 2015 IEEE 18th International Conference on Intelligent Transportation Systems*, Las Palmas de Gran Canaria, Spain, pp. 1143–1149, Sept. 2015. doi:[10.1109/ITSC.2015.189](https://doi.org/10.1109/ITSC.2015.189)

Delft Center for Systems and Control  
Delft University of Technology  
Mekelweg 2, 2628 CD Delft  
The Netherlands  
phone: +31-15-278.24.73 (secretary)  
URL: <https://www.dcsc.tudelft.nl>

---

\* This report can also be downloaded via [https://pub.bartdeschutter.org/abs/15\\_029](https://pub.bartdeschutter.org/abs/15_029)

# A new emission model including on-ramps for two-class freeway traffic control

C. Pasquale, S. Liu, S. Siri, S. Sacone, B. De Schutter

**Abstract**—The main objective of this paper is to propose a new two-class macroscopic emission model to describe the pollutant emissions produced by freeway traffic. The innovative aspect of the proposed model consists in considering the on-ramp emissions, which are explicitly modeled for different traffic scenarios. Next, a two-class local controller based on a ramp metering is reported with the aim of minimizing emissions and congestion in the freeway system. The relevance of the on-ramp emission model is in this way highlighted, since ramp metering may lead to creation of queues at the entering on-ramps and hence a concentration of pollutants on these on-ramps. Simulation results show the effectiveness of the proposed control strategy for a case of study.

## I. INTRODUCTION

The development of efficient freeway management tools has been, for several decades, an important research topic. Ramp metering is a widely proven control strategy, which regulates the access of traffic volumes to the mainstream freeway through traffic signals installed at the on-ramp [1]. The local feedback traffic controller ALINEA [2] and its extension to the proportional integral type version called PI-ALINEA [3], have been successfully applied in many real cases. Since then, more sophisticated control approaches have been developed in the literature in order to optimize the performances of the freeway system. For instance, in [4], [5] a nonlinear Model Predictive Control (MPC) scheme is applied for ramp metering, where the macroscopic METANET model [6] is adopted for traffic prediction. In other works, the control strategy is sought by solving a discrete-time constrained nonlinear optimal control problem (see [7] and the references therein), the numerical solution of which is hard to find by direct use of available nonlinear programming codes, due to the problem dimensions and complexity. An efficient numerical solution may be obtained using the feasible-direction algorithm that is adopted within the optimal freeway traffic control tool AMOC [8], [9]. More recent works propose sophisticated control architectures, based on AMOC, such as the three-layer hierarchical control approach described in [10] and the mainstream traffic flow control scheme proposed in [11].

Analyzing the literature, it is possible to observe that the traffic control approaches are often adopted in order to minimize the congestion and the total travel delay. However,

freeway control strategies may also be used to produce several benefits in terms of reductions in fuel consumption and emissions. Some recent works focus on this second aspect (see [12], [13], [14]), where the ramp metering control strategy, alone or combined with other traffic control measures (e.g. variable speed limits), is applied to minimize traffic emissions.

In the last years, several models have been defined in order to properly quantify and evaluate the emissions produced by vehicular traffic. Among others, the average-speed emission model COPERT proposed in [15] has already been adopted in [14], [16] for freeway control strategies. Other more accurate emission models, considering the emissions depending on both acceleration and speed, are present in the literature. For instance the VT-macro emission model has been proposed in [12], [17] in a single-class version and in [13] in a multi-class version. The more recent VERSIT+ emission model ([18], [19]), is able to compute different categories of pollutant emissions for many types of vehicles considering the combined effect of acceleration and speed and the driving behavior for different driving conditions.

In this paper, we consider a freeway traffic control approach that aims at minimizing traffic emissions and congestion, where a two-class macroscopic traffic flow model and a two-class local controller (allowing to devise separate control actions for the two vehicle classes) are considered. The main novelty of this work is to propose a new two-class macroscopic emission model, based on the microscopic VERSIT+ model, where the driving behavior on the on-ramp is explicitly modeled. Moreover the adopted local controller is based on the extension at the two-class case of the PI-ALINEA regulator, where the gain parameters and the set-point are sought by solving a finite horizon optimization problem (FHOP), which minimizes emission and congestion in different traffic conditions. It is important to note that the controller can be recalibrated offline or online, using the two-class traffic model and the new two-class emission model. In the literature similar tuning approaches are reported in [20], [21].

This paper is organized as follows. The two-class traffic model is described in Section II, the microscopic VERSIT+ emission model is introduced in Section III, whereas the new two-class macroscopic VERSIT+ emission model is proposed and described in Section IV. The adopted two-class ramp metering local control strategy is described in Section V, where some useful key performance parameters are also reported. The simulation results are discussed in Section VI. Final conclusions are drawn in Section VII.

C. Pasquale, S. Sacone, S. Siri are with the Department of Informatics, Bioengineering, Robotics and Systems Engineering, University of Genova, Italy.

S. Liu, B. De Schutter are with the Delft Center for Systems and Control, Delft University of Technology, The Netherlands.

For the research leading to these results, Shuai Liu has received funding from the China Scholarship Council.

## II. THE TWO-CLASS METANET MODEL

In this work a two-class version of the METANET macroscopic traffic model is considered. The freeway stretch is divided in  $N$  sections and the time horizon is discretized in  $K$  time steps and  $c = 1, 2$  represents the vehicle class ( $c = 1$  represents the class of cars whereas  $c = 2$  indicates the class of trucks). Moreover, let  $T$  indicate the sample time interval and  $L_i$  the length of section  $i$ .

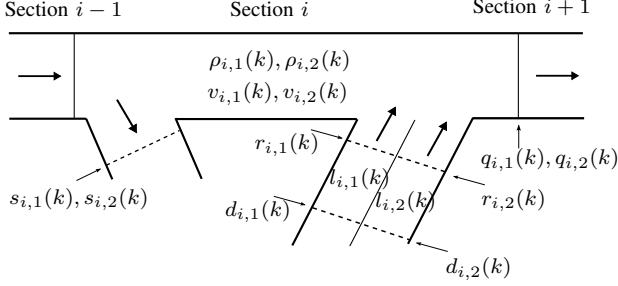


Fig. 1: The two-class model variables.

The traffic dynamics in the freeway stretch is given by the evolution of the main aggregate variables defined for each section  $i$  and for class  $c$  (see also Fig. 1): the traffic density  $\rho_{i,c}(k)$  (expressed in [veh/km]), the mean traffic speed  $v_{i,c}(k)$  (expressed in [km/h]), the traffic outflow  $q_{i,c}(k)$  (expressed in [veh/h]) and the queue length of vehicles waiting on the on-ramp  $l_{i,c}(k)$  (expressed in [veh]). Let us also introduce the on-ramp traffic volume  $r_{i,c}(k)$ , the off-ramp traffic volume  $s_{i,c}(k)$  and the traffic demand  $d_{i,c}(k)$  ([veh/h]). The considered model includes some traffic parameters. Specifically, for section  $i$ ,  $v_{i,c}^f$  is the free-flow speed for class  $c$ ,  $\rho_i^{cr}$  is the critical density,  $\rho_i^{\max}$  is the jam density,  $r_{i,c}^{\max}$  is the on-ramp capacity for class  $c$ . Moreover, the parameter  $\eta$  is a conversion factor between vehicles of class 1 and 2 whose meaning is analogous to the definition of passenger car equivalent (PCE).

The two-class model equations are

$$\rho_{i,c}(k+1) = \rho_{i,c}(k) + \frac{T}{L_i} \left[ q_{i-1,c}(k) - q_{i,c}(k) + r_{i,c}(k) - s_{i,c}(k) \right] \quad (1)$$

$$v_{i,c}(k+1) = v_{i,c}(k) + \frac{T}{\tau_c} \left[ V_{i,c}(k) - v_{i,c}(k) \right] + \frac{T}{L_i} v_{i,c}(k) (v_{i-1,c}(k) - v_{i,c}(k)) - \frac{\nu_c T (\rho_{i+1}(k) - \rho_i(k))}{\tau_c L_i (\rho_i(k) + \chi_c)} - \delta_c^{\text{on}} T \frac{v_{i,c}(k) r_i(k)}{L_i (\rho_i(k) + \chi_c)} \quad (2)$$

$$l_{i,c}(k+1) = l_{i,c}(k) + T [d_{i,c}(k) - r_{i,c}(k)] \quad (3)$$

with  $q_{i,c}(k) = \rho_{i,c}(k) \cdot v_{i,c}(k)$ ,  $c = 1, 2$ ,  $i = 1, \dots, N$ ,  $k = 0, \dots, K-1$  and where  $\tau_c$ ,  $\nu_c$ ,  $\chi_c$ ,  $\delta_c^{\text{on}}$ , are suitable parameters.

The steady-state speed density relation  $V_{i,c}(k)$  in (2) can be expressed as:

$$V_{i,c}(k) = v_{i,c}^f \cdot \left[ 1 - \left( \frac{\rho_i(k)}{\rho_i^{\max}} \right)^{l_c} \right]^{m_c} \quad (4)$$

with  $c = 1, 2$ ,  $k = 0, \dots, K-1$  and where  $l_c$ ,  $m_c$ , are model parameters specific for each vehicle class. To properly consider the interaction between the two classes of vehicles, the total density and the total on-ramp traffic volume are introduced in (2) and for  $i = 1, \dots, N$  and  $k = 0, \dots, K-1$  can be computed as

$$\rho_i(k) = \rho_{i,1}(k) + \eta \rho_{i,2}(k) \quad (5)$$

$$r_i(k) = r_{i,1}(k) + \eta r_{i,2}(k) \quad (6)$$

In case the freeway system is not controlled, the on-ramp entering flow can be computed as follows

$$r_{i,c}(k) = \min \left\{ d_{i,c}(k) + \frac{l_{i,c}(k)}{T}, r_{i,c}^{\max}, r_{i,c}^{\max} \cdot \frac{\rho_i^{\max} - \rho_i(k)}{\rho_i^{\max} - \rho_i^{cr}} \right\} \quad (7)$$

The flows entering the first section from the mainstream are computed similarly to on-ramps flows.

In case the on-ramps are controlled via ramp metering and letting  $\bar{r}_{i,c}(k)$  denote the actuated on-ramp flow for section  $i = 1, \dots, N$ , at time step  $k = 0, \dots, K-1$  for class  $c = 1, 2$ , (7) are substituted by

$$r_{i,c}(k) = \min \left\{ d_{i,c}(k) + \frac{l_{i,c}(k)}{T}, \bar{r}_{i,c}(k), r_{i,c}^{\max}, r_{i,c}^{\max} \cdot \frac{\rho_i^{\max} - \rho_i(k)}{\rho_i^{\max} - \rho_i^{cr}} \right\} \quad (8)$$

## III. THE VERSIT+ EMISSION MODEL

In order to properly consider the freeway traffic emissions, the microscopic emission model VERSIT+ (for details see [18]) will be considered. This model is able to compute many types of pollutant emissions for a wide range of vehicles and for several traffic conditions. In particular the emission factor, produced by the model, depends in part on the combination of acceleration and speed, included in the model by the dynamic variable  $w = a + 0.014v$  and in part on the value of the speed, which may be divided in four categories corresponding to different driving conditions: idling condition with  $v < 5$  and  $a < 0.5$ , urban driving with  $v \leq 50$ , rural driving with  $50 < v \leq 80$  and motorway driving with  $v > 80$ . The emission factor  $E$  in [g/s] is given by

$$E = \begin{cases} u_0 & \text{if } v < 5 \text{ and } a < 0.5 \\ u_1 + u_2 w_+ + u_3 (w - 1)_+ & \text{if } v \leq 50 \\ u_4 + u_5 w_+ + u_6 (w - 1)_+ & \text{if } 50 < v \leq 80 \\ u_7 + u_8 (w - 0.5)_+ + u_9 (w - 1.5)_+ & \text{if } v > 80 \end{cases} \quad (9)$$

where  $a$  represents the acceleration of vehicles in [ $\text{m/s}^2$ ] and  $v$  represents the speed in [km/h], whereas  $u_j$ ,  $j =$

$0, \dots, 9$ , are the coefficients of the emission model for each driving condition. Moreover the function  $(x)_+$  imposes the nonnegativity of the variable  $x$ :

$$(x)_+ = \begin{cases} 0 & \text{if } x < 0 \\ x & \text{otherwise} \end{cases} \quad (10)$$

#### IV. THE NEW TWO-CLASS MACROSCOPIC VERSIT+ EMISSION MODEL

A new version of the macroscopic VERSIT+ emission model is described in the present section.

##### A. The mainstream emission

In order to adopt the VERSIT+ emission model, the average acceleration and the number of vehicles involved have to be computed for each section  $i$ , for each class of vehicles  $c$  and for every simulation time step  $k$ . In [12], [17], two types of acceleration have been identified: the segmental acceleration considering the speed variation within a section, and the cross-segmental acceleration, which concerns the speed variation of vehicles moving from one section to the consecutive one between time step  $k$  and  $k + 1$ . In [13], [22] such accelerations have been extended to the multi-class case, and in [19] a multi-class version of VERSIT+ emission model has been proposed. In the following  $a_{i,c}^{\text{seg}}(k)$  and  $a_{i,i+1,c}^{\text{cross}}(k)$  are reported, adapted to the two-class model considered in this paper, i.e.

$$a_{i,c}^{\text{seg}}(k) = \frac{v_{i,c}(k+1) - v_{i,c}(k)}{T} \quad (11)$$

$$a_{i,i+1,c}^{\text{cross}}(k) = \frac{v_{i+1,c}(k+1) - v_{i,c}(k)}{T} \quad (12)$$

with  $c = 1, 2$ ,  $i = 1, \dots, N$ ,  $k = 0, \dots, K - 1$ .

Moreover, the number of vehicles  $n_{i,c}^{\text{seg}}(k)$  and  $n_{i,i+1,c}^{\text{cross}}(k)$  subject to segmental and cross-segmental accelerations, are respectively given by

$$n_{i,c}^{\text{seg}}(k) = L_i \rho_{i,c}(k) - T q_{i,c}(k) \quad (13)$$

$$n_{i,i+1,c}^{\text{cross}}(k) = T q_{i,c}(k) \quad (14)$$

with  $c = 1, 2$ ,  $i = 1, \dots, N$ ,  $k = 0, \dots, K - 1$ .

##### B. The on-ramp emission

In the existing works, the emissions of vehicles present on the on-ramps have not been considered. Nevertheless, the operating conditions of such vehicles are quite important and the associated emissions should be included in the total calculation of traffic emissions. In this work, in order to consider the driving behavior on the on-ramp, four groups of vehicles (i.e. arriving vehicles, waiting vehicles, leaving vehicles with stop and leaving vehicles without stop) are introduced.

The arriving vehicles represent the vehicles arriving at the on-ramp at time step  $k$  and waiting at time step  $k + 1$ . Such vehicles are subject to the arriving acceleration

$$a_{i,c}^{\text{a}}(k) = \frac{v_{i,c}^{\text{idl}}(k+1) - v_{i,c}^{\text{on}}(k)}{T} \quad (15)$$

where  $v_{i,c}^{\text{on}}(k)$  is the on-ramp speed and  $v_{i,c}^{\text{idl}}(k)$  is the speed of the vehicles moving within the queue. Both speeds are assumed to be based on on-line measurements.

The waiting vehicles, representing the vehicles moving within the queue on the on-ramp between time step  $k$  and time step  $k + 1$ , have the following acceleration

$$a_{i,c}^{\text{w}}(k) = \frac{v_{i,c}^{\text{idl}}(k+1) - v_{i,c}^{\text{idl}}(k)}{T} \quad (16)$$

The acceleration of leaving vehicles with stop, representing the vehicles at the head of the queue at time step  $k$  and that leave the on-ramp at time step  $k + 1$ , is computed as

$$a_{i,c}^{\text{ls}}(k) = \frac{v_{i,c}(k+1) - v_{i,c}^{\text{idl}}(k)}{T} \quad (17)$$

The leaving vehicles without stop, representing the vehicles that arrive at the on-ramp at time step  $k$  and leave the on-ramp at time step  $k + 1$  without any intermediate stops, are characterized by the following acceleration

$$a_{i,c}^{\text{lns}}(k) = \frac{v_{i,c}(k+1) - v_{i,c}^{\text{on}}(k)}{T} \quad (18)$$

with  $c = 1, 2$ ,  $i = 1, \dots, N$ ,  $k = 0, \dots, K - 1$ . The number of vehicles belonging to each group may be defined according to the entering flow from the on-ramp  $r_{i,c}(k)$  at time step  $k$ . To this end, the following two scenarios may be distinguished:

- scenario 1 with  $0 \leq r_{i,c}(k) \leq \frac{l_{i,c}(k)}{T}$ ;
- scenario 2 with  $\frac{l_{i,c}(k)}{T} < r_{i,c}(k) \leq d_{i,c}(k) + \frac{l_{i,c}(k)}{T}$ .

Fig. 2 and Fig. 3 depict the driving behavior in these two scenarios, while Fig. 4 illustrates the patterns used to indicate the number of arriving vehicles  $n_{i,c}^{\text{a}}(k)$ , the number of waiting vehicles  $n_{i,c}^{\text{w}}(k)$ , the number of leaving vehicles with stop  $n_{i,c}^{\text{ls}}(k)$ , and the number of leaving vehicles without stop  $n_{i,c}^{\text{lns}}(k)$ . In the first scenario (Fig. 2) the following equations are used

$$n_{i,c}^{\text{a}}(k) = T d_{i,c}(k) \quad (19)$$

$$n_{i,c}^{\text{w}}(k) = l_{i,c}(k) - T r_{i,c}(k) \quad (20)$$

$$n_{i,c}^{\text{ls}}(k) = T r_{i,c}(k) \quad (21)$$

$$n_{i,c}^{\text{lns}}(k) = 0 \quad (22)$$

with  $c = 1, 2$ ,  $i = 1, \dots, N$ ,  $k = 0, \dots, K - 1$ .

In the second scenario (Fig. 3), instead, the following equations hold

$$n_{i,c}^{\text{a}}(k) = T d_{i,c}(k) + l_{i,c}(k) - T r_{i,c}(k) \quad (23)$$

$$n_{i,c}^{\text{w}}(k) = 0 \quad (24)$$

$$n_{i,c}^{\text{ls}}(k) = l_{i,c}(k) \quad (25)$$

$$n_{i,c}^{\text{lns}}(k) = T r_{i,c}(k) - l_{i,c}(k) \quad (26)$$

with  $c = 1, 2$ ,  $i = 1, \dots, N$ ,  $k = 0, \dots, K - 1$ .

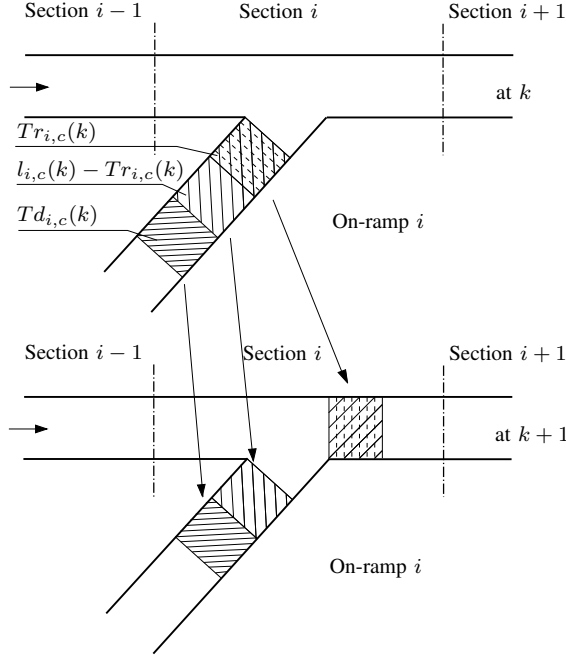


Fig. 2: Dynamic behavior of vehicles at the on-ramp in Scenario 1

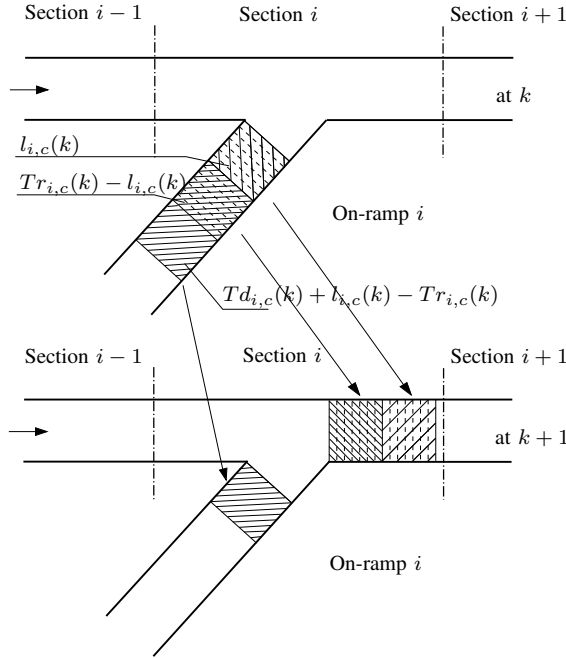


Fig. 3: Dynamic behavior of vehicles at the on-ramp in Scenario 2

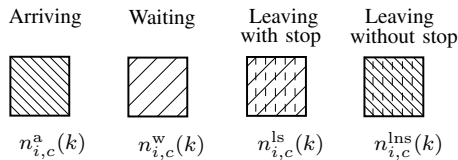


Fig. 4: Legend for Figs. 2 and 3

### C. Overall two-class VERSIT+ model

In accordance with the accelerations previously defined, the two-class macroscopic VERSIT+ emission model, for each vehicle class  $c$ , for each section  $i$  and for each time step  $k$ , may be computed using equation (9) and replacing the variables as indicated in Table I.

TABLE I: Variables definition of the two-class VERSIT+ model.

VERSIT+	Two-class VERSIT+		
$E$	$E_{i,c}^{\text{seg}}$	$E_{i,i+1,c}^{\text{cross}}$	$E_{i,c}^{\text{ramp},y}$
$w$	$w_{i,c}^{\text{seg}}$	$w_{i,i+1,c}^{\text{cross}}$	$w_{i,c}^y$
$v$	$v_{i,c}$	$v_{i,c}$	$v_{i,c}^y$
$a$	$a_{i,c}^{\text{seg}}$	$a_{i,i+1,c}^{\text{cross}}$	$a_{i,c}^y$

The coefficients  $u_j$ ,  $j = 0, \dots, 9$ , used in (9), are replaced by the coefficients  $u_{j,i,c}$ ,  $j = 0, \dots, 9$ , properly identified for the two-class emission model for each section  $i$  and vehicle class  $c$ , whereas  $y \in \{a, w, ls, lns\}$ , and  $v_{i,c}^y(k)$  assumes the following values

$$v_{i,c}^y(k) = \begin{cases} v_{i,c}^{\text{on}}(k) & \text{if } y = a, \text{ or } y = lns \\ v_{i,c}^{\text{idl}}(k) & \text{if } y = w, \text{ or } y = ls \end{cases} \quad (27)$$

## V. THE TWO-CLASS PI-ALINEA CONTROL STRATEGY

The local ramp metering strategies adopted in this work originate from the well-known controller ALINEA [2], which has shown, also in real applications, to be a simple and effective control strategy [23]. In particular the considered controllers are based on the two-class PI-ALINEA proposed in [16] in which two different control actions are applied for cars and trucks waiting in separate lanes at the on-ramps. Let us first of all define the following quantities indicating the ratio of the occupancy of each class over the entire occupancy (including both the mainstream and the queues)

$$f_{i,1}(k) = \frac{o_{i,1}(k)L_i + l_{i,1}(k)}{o_{i,1}(k)L_i + l_{i,1}(k) + \eta \cdot [o_{i,2}(k)L_i + l_{i,2}(k)]} \quad (28)$$

$$f_{i,2}(k) = \frac{\eta \cdot [o_{i,2}(k)L_i + l_{i,2}(k)]}{o_{i,1}(k)L_i + l_{i,1}(k) + \eta \cdot [o_{i,2}(k)L_i + l_{i,2}(k)]} \quad (29)$$

Hence, the on-ramp flow of class  $c$  is set as follows

$$\bar{r}_{i,c}(k) = \max \left\{ r_{i,c}^{\min}, r_{i,c}(k-1) - K_{Pc}[o_{i,c}(k-1) - o_{i,c}(k-2)] + K_{Rc} \cdot f_{i,c}(k-1)[\hat{o} - o_i(k-1)] \right\} \\ c = 1, 2, \quad i = 1, \dots, N, \quad k = 0, \dots, K-1 \quad (30)$$

where  $\hat{o}$  is the occupancy set-point appropriately defined to reduce pollutant emissions and congestion,  $K_{Pc}$  and  $K_{Rc}$ ,  $c = 1, 2$ , are suitable parameters for the considered

regulators,  $r_{i,c}^{\min}$  is the minimum on-ramp traffic volume for class  $c$  and on-ramp  $i$  and the total occupancy is obtained as

$$o_i(k) = o_{i,1}(k) + \eta o_{i,2}(k) \quad i = 1, \dots, N, \quad k = 0, \dots, K-1 \quad (31)$$

It is worth nothing that the values of the occupancy measurements are typically given as percentages or as values between 0 and 1. In this paper we assume that these values are reported to a density scale and expressed in [veh/km].

In order to evaluate the effectiveness of the proposed control strategy, some performance indicators are introduced. These indicators show the effects in terms of reduction of traffic emissions and in terms of reduction of congestion (i.e., maximization of the throughput) on the whole time horizon and on the entire freeway stretch.

Let us start from the indicators of traffic emissions. The total emissions in the freeway, denoted as TE and expressed in [g], may be computed by adopting the relations of the extended VERSIT+ emission model described in Section IV-C, and are given by

$$\begin{aligned} \text{TE} = & \sum_{k=1}^K \sum_{i=1}^N \sum_{c=1}^2 T \left[ E_{i,c}^{\text{seg}}(k) \cdot n_{i,c}^{\text{seg}}(k) \right. \\ & \left. + E_{i,i+1,c}^{\text{cross}}(k) \cdot n_{i,i+1,c}^{\text{cross}}(k) + \sum_{y \in \{a, w, ls, lns\}} E_{i,c}^{\text{ramp},y}(k) \cdot n_{i,c}^y(k) \right] \quad (32) \end{aligned}$$

Besides the emissions in the freeway, other important indexes regard the capability of the control scheme to reduce the congestion and to improve traffic conditions. In the following, the two most common performance indexes adopted in literature (see for instance [24]) are described, properly adapted to the two-class case. The Total Time Spent (TTS), in [veh·h], is computed as

$$\begin{aligned} \text{TTS} = & \sum_{k=1}^K \sum_{i=1}^N T \left[ L_i \left( \rho_{i,1}(k) + \eta \cdot \rho_{i,2}(k) \right) \right. \\ & \left. + \left( l_{i,1}(k) + \eta \cdot l_{i,2}(k) \right) \right] \quad (33) \end{aligned}$$

The Total Traveled Distance (TTD), measured in [veh·km], is given by

$$\text{TTD} = \sum_{k=1}^K \sum_{i=1}^N \left[ L_i \cdot T \left( q_{i,1}(k) + \eta \cdot q_{i,2}(k) \right) \right] \quad (34)$$

As introduced previously, the two-class PI-ALINEA parameters have to be properly calibrated in order to reduce congestion and at the same time to minimize the total emissions. At this purpose, a finite horizon optimization problem is proposed in order to define the optimal value of the desired density  $\hat{o}$ , and the optimal values of the gain factors  $K_{Pc}$  and  $K_{Rc}$ ,  $c = 1, 2$ . The FHOP is stated with reference to a time horizon denoted with  $\bar{K}$ , to initial traffic conditions, and to proper estimates of the traffic demands over the given time horizon. By considering a generic time step  $k$ , the problem statement follows:

*Problem 1:* Given the system initial conditions  $\rho_{i,c}(k)$ ,  $v_{i,c}(k)$ ,  $l_{i,c}(k)$ ,  $i = 1, \dots, N$ ,  $c = 1, 2$ , the present traffic demand  $d_{i,c}(k)$  and the estimated values  $d_{i,c}(h)$ ,  $i = 0, \dots, N$ ,  $c = 1, 2$ ,  $h = k + 1, \dots, k + \bar{K}$ , find the PI-ALINEA parameters  $\hat{o}$ ,  $K_{Pc}$  and  $K_{Rc}$ ,  $c = 1, 2$ , which minimize

$$\alpha \cdot \frac{\text{TE}}{\text{TTS} + \text{TE}} + (1 - \alpha) \cdot \frac{\text{TTS}}{\text{TTS} + \text{TE}} \quad (35)$$

with the TE and TTS being computed in the time interval  $[kT, (k + \bar{K})T]$  and subject to the two-class METANET traffic flow model, the two-class VERSIT+ emission model, and the two-class PI-ALINEA control strategy.  $\square$

In the proposed objective function, TE and TTS are arbitrarily weighted by  $\alpha \in [0, 1]$ . The FHOP is a nonlinear optimization problem that may be applied in different ways, both in online and in offline schemes.

Specifically, in an offline scheme, a set of suitable traffic scenarios (characterized by different initial conditions and estimates of the demands) is defined, and the FHOP is solved for each scenario, finding the corresponding parameters of the PI-ALINEA regulator. Then, in the real-time application of the control strategy, the most suitable scenario is identified and the corresponding parameters are applied.

Alternatively, the FHOP can be solved on-line, on the basis of the measured system state and the estimated demands. Then, whenever it happens that the traffic demand has a behavior significantly different from the expected one, the FHOP is solved again and new regulator parameters are computed and applied.

## VI. SIMULATION RESULTS

In the following, simulation results are proposed in which the uncontrolled scenario is compared with the controlled one. In particular the proposed two-class PI-ALINEA regulator is used in order to reduce the congestion and the emissions in the considered freeway stretch. To this end, the two-class macroscopic VERSIT+ model is adopted to compute the CO<sub>2</sub> emissions. The considered case study concerns a three-lane freeway stretch composed of  $N = 20$  sections, each one with a length  $L_i = 500$  [m], with three on-ramps located in sections  $i = 12, 14, 16$  (see Fig. 5). The sample time is  $T = 10$  [s] and a total time horizon of 2 and half hours ( $K = 900$ ) is considered for the simulation tests. The case study is characterized by trapezoidal demand profiles for both vehicle classes, as shown in the left side plots in Fig. 6, whereas the mainstream flow is considered constant for total time horizon and is composed of 4000 cars per hour and 186 trucks per hour. For this case study the following traffic model parameters are selected:  $v_{i,1}^f = 120$  [km/h],  $v_{i,2}^f = 90$  [km/h],  $\rho_i^{\max} = 200$  [veh/km/lane],  $\rho_i^{\text{cr}} = 46.66$  [veh/km/lane],  $r_{i,1}^{\max} = 1800$  [veh/h],  $r_{i,2}^{\max} = 450$  [veh/h],  $\forall i$ , and the conversion factor  $\eta$  has been chosen equal to 4. As regards the VERSIT+ emission model, the on-ramp speed  $v_{i,c}^{\text{on}}(k)$  is considered constant and selected equal to 30 [km/h], and the speed of the vehicles moving within

the queue  $v_{i,c}^{\text{idl}}(k)$  is also considered constant and equal to 5 [km/h],  $\forall i$ .

#### A. Uncontrolled case

Referring to the plots on the right side of Fig. 6 showing the behavior of density downstream the three on-ramps, it is possible to observe that the uncontrolled case is characterized by a high congestion in the downstream sections, in which for most of the time the density is much higher than the critical value. In the uncontrolled case the queue lengths at the on-ramps are zero over the whole simulation horizon. Fig. 7a depicts the density evolution in all sections in the uncontrolled case. Referring to this figure it is evident that the level of congestion is quite high when no control is applied. Finally, Fig. 7b describes the CO<sub>2</sub> evolutions in space and time in the case without control. The resulting Total Time Spent is  $\text{TTS} = 2613$  [veh·h], the Total Emissions are  $\text{TE} = 33357$  [kg] and the Total Travel Distance is  $\text{TTD} = 152156$  [veh· km].

#### B. Controlled case

In order to apply the two-class PI-ALINEA strategy, Problem 1 has been solved considering the estimated traffic demand over the whole time period and choosing the weight parameter  $\alpha$  equal to 0.5. In the present proposal, the considered scenarios correspond to regular traffic conditions and to possibly critical conditions in the time intervals between the beginning and the end of peak periods. This means that the regulator parameters are changed just at the beginning and at the end of rush hours. The obtained gain factors are  $K_{P1} = 100$ ,  $K_{P2} = 50$ ,  $K_{R1} = 30$ ,  $K_{R2} = 5$  [km/h] whereas the optimal occupancy set-point  $\hat{o}$ , converted to a density scale, is 47 [veh/km/lane]. The results obtained by applying the two-class PI-ALINEA controller are presented below. Fig. 8 shows, on the right side, the density behavior downstream of the on-ramps, which is strongly reduced by applying the proposed control strategy. However, it is also possible to observe that the control approach causes the creation of a queue at the third on-ramp (left side of Fig. 8), whereas the queues at the others on-ramp are zero due to the local nature of the controller. Moreover, the TTS is reduced to 2223 [veh·h], which is a 14.93% reduction compared with the uncontrolled case, TE is reduced to 28011 [kg], which is a 16.03% reduction compared with the uncontrolled case, whereas the TTD is very close to the uncontrolled case, corresponding to 0.098%. These results are confirmed by Fig. 9a and by Fig. 9b. In particular, Fig. 9a shows a strong reduction of the congestion compared with the uncontrolled case depicted in Fig. 7a, whereas Fig. 9b illustrates the global reduction of CO<sub>2</sub> emissions, which are more concentrated on the freeway section corresponding to the third on-ramp, since vehicles are queued on this on-ramp as a consequence of the application of the two-class PI-ALINEA.

### VII. CONCLUSIONS

In this paper a new two-class macroscopic emission model has been proposed able to model several types of pollutant

emissions produced on the freeway by cars and trucks. In this model, the driving behavior at the on-ramps has been included in order to properly calculate the emissions produced on the on-ramps in different traffic scenarios. Finally, a ramp metering control strategy based on the two-class PI-ALINEA controller has been proposed in order to reduce emissions and congestion through a proper parameter optimization of the two-class controller. The effectiveness of the proposed control strategy has been confirmed by simulation results in which it is shown that, for the considered scenario, reduction of emissions and maximization of the throughput are nonconflicting objectives, since both the total emissions and the congestion are reduced if the control action is applied. Furthermore, the results show that the adoption of ramp metering control laws may cause a high concentration of pollutants at the entering on-ramps. As a consequence, the effect of these emissions cannot be excluded in the global computation, since these may be harmful for the environment, especially if the on-ramps are located in proximity of urban areas.

### REFERENCES

- [1] M. Papageorgiou and I. Papamichail, "Overview of traffic signal operation policies for ramp metering," *Transportation Research Record: Journal of the transportation research board*, vol. 2047, no. 1, pp. 28–36, 2008.
- [2] M. Papageorgiou, H. Hadj-Salem, and J.-M. Blosseville, "ALINEA: A local feedback control law for on-ramp metering," *Transportation Research Record*, no. 1320, pp. 58–64, 1991.
- [3] Y. Wang, M. Papageorgiou, J. Gaffney, I. Papamichail, and J. Guo, "Local ramp metering in the presence of random-location bottlenecks downstream of a metered on-ramp," in *Proc. of the 13th IEEE Conference on Intelligent Transportation Systems*, pp. 1462–1467, 2010.
- [4] A. Hegyi, B. D. Schutter, and H. Hellendoorn, "Model predictive control for optimal coordination of ramp metering and variable speed limits," *Transportation Research Part C*, vol. 13, no. 3, pp. 185–209, 2005.
- [5] T. Bellemans, B. D. Schutter, and B. D. Moor, "Model predictive control for ramp metering of motorway traffic: A case study," *Control Engineering Practice*, vol. 14, no. 7, pp. 757–767, 2006.
- [6] M. Papageorgiou, J.-M. Blosseville, and H. Hadj-Salem, "Modelling and real-time control of traffic flow on the southern part of boulevard peripherique in paris: Part i: Modelling," *Transportation Research Part A*, vol. 24, no. 5, pp. 345–359, 1990.
- [7] A. Kotsialos, M. Papageorgiou, M. Mangeas, and H. Haj-Salem, "Coordinated and integrated control of motorway networks via nonlinear optimal control," *Transportation Research Part C*, vol. 10, no. 1, pp. 65–84, 2002.
- [8] A. Kotsialos, M. Papageorgiou, and F. Middelham, "Optimal coordinated ramp metering with AMOC," *Transportation Research Record*, vol. 1748, pp. 55–65, 2001.
- [9] M. Papageorgiou and A. Kotsialos, "Nonlinear optimal control applied to coordinated ramp metering," *IEEE Transactions on Control Systems Technology*, vol. 12, no. 6, pp. 920–933, 2004.
- [10] I. Papamichail, A. Kotsialos, I. Margonis, and M. Papageorgiou, "Coordinated ramp metering for freeway networks—a model-predictive hierarchical control approach," *Transportation Research Part C*, vol. 18, no. 3, pp. 311–331, 2010.
- [11] R. Carlson, I. Papamichail, M. Papageorgiou, and A. Messmer, "Optimal mainstream traffic flow control of large-scale motorway networks," *Transportation Research Part C*, vol. 18, no. 2, pp. 193–212, 2010.
- [12] S. Zegheye, B. De Schutter, J. Hellendoorn, E. Breunesses, and A. Hegyi, "Integrated macroscopic traffic flow, emission, and fuel consumption model for control purposes," *Transportation Research Part C*, vol. 31, pp. 158–171, 2013.

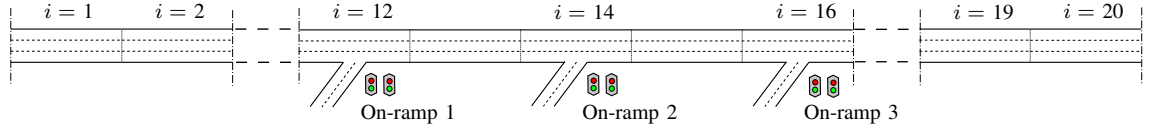


Fig. 5: Layout of the considered freeway stretch.

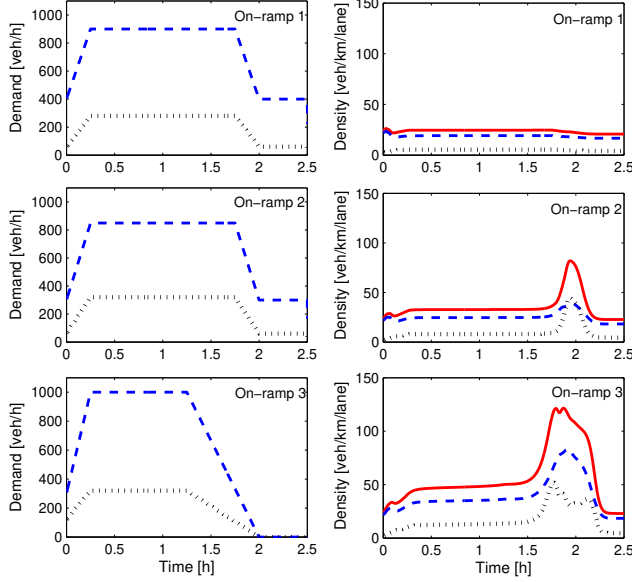


Fig. 6: Uncontrolled case (dashed blue line for cars, dotted black line for trucks [PCE], solid red line for cars plus trucks [PCE]).

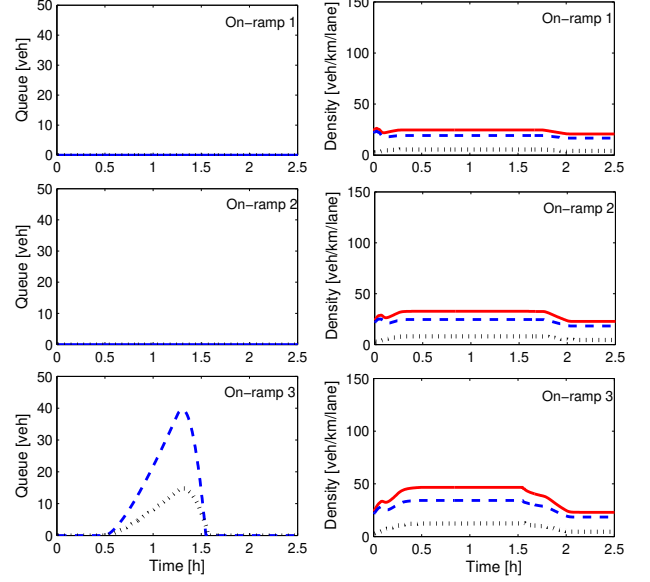


Fig. 8: Controlled case (dashed blue line for cars, dotted black line for trucks [PCE], solid red line for cars plus trucks [PCE]).

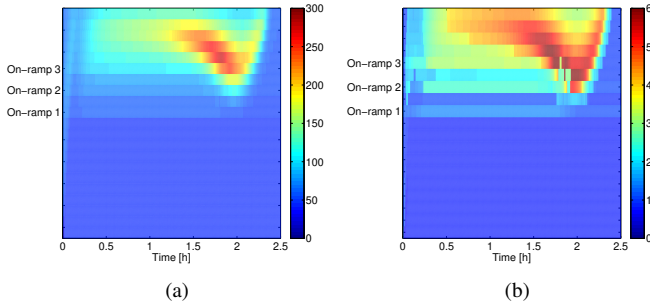


Fig. 7: Mainstream density (7a) and total CO<sub>2</sub> emissions (7b) in the uncontrolled case.

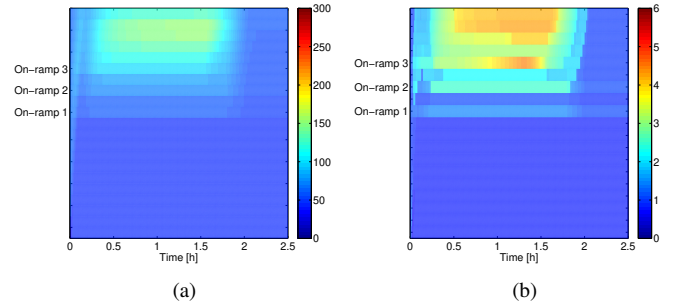


Fig. 9: Mainstream density (9a) and total CO<sub>2</sub> emissions (9b) in the controlled case.

- [13] S. Liu, B. De Schutter, and H. Hellendoorn, "Integrated traffic flow and emission control based on FASTLANE and the multi-class VT-macro model," in *Proc. of the 2014 European Control Conference*, 2014.
- [14] C. Pasquale, S. Saccone, and S. Siri, "Two-class emission traffic control for freeway systems," in *Proc. of the 19th IFAC World Congress*, pp. 936–941, 2014.
- [15] L. Ntziachristos and C. Kouridis, "Road transport emission chapter of the EMEP/CORINAIR emission inventory guidebook," *European Environment Agency Technical Report*, no. 16, 2007.
- [16] C. Pasquale, S. Saccone, and S. Siri, "Ramp metering control for two vehicle classes to reduce traffic emissions in freeway systems," in *Proc. of the European Control Conference*, pp. 2588–2593, 2014.
- [17] S. Zegeye, B. De Schutter, J. Hellendoorn, E. Breunese, and A. Hegyi, "A predictive traffic controller for sustainable mobility using parameterized control policies," *IEEE Transactions on Intelligent Transportation Systems*, vol. 13, no. 3, pp. 1420–1429, 2012.
- [18] N. E. Ligterink, R. D. Lange, and E. Schoen, "Refined vehicle and driving-behavior dependencies in the VERSIT+ emission model," in *Proc. of the ETAPP Symposium*, pp. 177–186, 2009.
- [19] S. Liu, B. De Schutter, and H. Hellendoorn, "Model predictive control based on multi-class traffic models," tech. rep., Delft Center for Systems and Control, Delft University of Technology, 2014.
- [20] L. Chu and X. Yang, "Optimization of the ALINEA ramp-metering control using genetic algorithm with micro-simulation," in *Transportation Research Board 82nd Annual Meeting Compendium of Papers*,



2003.

- [21] S. Jin, Z. Hou, R. Chi, and J. Hao, "A data-driven control design approach for freeway traffic ramp metering with virtual reference feedback tuning," *Mathematical Problems in Engineering*, 2014.
- [22] S. Liu, B. De Schutter, and H. Hellendoorn, "Multi-class traffic flow and emission control for freeway networks," in *Proc. of the 16th International IEEE Conference on Intelligent Transportation Systems*, pp. 2223–2228, 2013.
- [23] M. Papageorgiou, E. Kosmatopoulos, I. Papamichail, and Y. Wang, "ALINEA maximises motorway throughput-an answer to flawed criticism," *Traffic Engineering and Control*, vol. 48, pp. 271–276, 2007.
- [24] H. Haj-Salem and M. Papageorgiou, "Ramp metering impact on urban corridor traffic: Field results," *Transportation Research Part A*, vol. 29, pp. 303–319, 1995.